

# THE EFFECT OF BAND ENGINEERING OF SEMICONDUCTORS ON PHOTOCATALYTIC WATER SPLITTING: A REVIEW

Lee Chung Lau<sup>1</sup>, KeatTeong Lee<sup>2</sup>

<sup>1,2</sup>School of Chemical Engineering, Universiti Sains Malaysia, Engineering Campus, Seri Ampangan, 14300 Nibong Tebal, Pulau Pinang, Malaysia, [chktee@eng.usm.my](mailto:chktee@eng.usm.my)

## Abstract

The direct conversion of solar energy using a photocatalyst in a water splitting reaction is a source of a sustainable and clean hydrogen supply. In general, photocatalysts are semiconductors that possess valence and conduction bands. These energy bands permit the absorption of photon energy to excite electrons in the outer orbitals of the photocatalysts. Photoexcited electron and hole pairs can subsequently induce a watersplitting reaction to produce hydrogen and oxygen. Photocatalytic water splitting is affected by the band level and crystallinity of the photocatalyst. Therefore, band engineering using chemical modifications such as cationic and anionic modification could create a photocatalyst suitable for the large-scale production of hydrogen. In this paper, cationic and anionic modifications of photocatalysts and the effects of these modifications on photocatalytic water splitting are reviewed.

**Keywords:** Water splitting; Photocatalysis; Hydrogen

\*\*\*

## 1. INTRODUCTION

The growth of energy consumption worldwide has resulted in an intensified use of fossil fuels. The resulting pollutants produced during fossil fuel combustion and the depletion of fossil fuels has encouraged a search for alternative and renewable energy sources that will enhance both energy security and environmental protection. The direct conversion of solar energy into usable energy has been a promising solution to the problem. Among various solar energy technologies, photocatalytic water splitting has been studied rigorously, especially after the discovery of Honda and Fujishima in 1972[1]. The photocatalytic water splitting reaction evolves hydrogen, which is a form of clean energy that produces no pollutants during combustion. In conjunction with the development of fuel cell technology, transformation into a hydrogen-based economy could be realized in the near term, if an inexpensive and carbon-neutral source of hydrogen is developed. A photocatalyst that could induce photocatalytic water splitting has properties similar to a semiconductor. A photocatalyst can form a conduction band and a valence band when the electrons located in the outer orbitals are excited by photons from light irradiation. These excited electrons will move into the conduction band while the valence band will contain holes where the electrons were originally located. These electron-hole pairs can subsequently react with surrounding substrates, such as with a water molecule in a redox reaction. A photoexcited electron will reduce a water molecule into hydrogen whereas a hole will oxidize the water molecule to produce oxygen. In reality, not all electron-hole pairs can induce water splitting because of electron-hole recombination. Hydrogen or oxygen evolution is thermodynamically possible only if the potential of the

conduction band is more negative than 0 V at NHE and if that of the valence band is more positive than 1.23 V at NHE, as illustrated in Fig. 1. For an overall water splitting reaction, (i.e., hydrogen and oxygen evolve at a stoichiometric ratio), the band gap of the photocatalyst must be at least 1.23 V, which corresponds to light irradiation of 1100 nm and indicates the possibility of using visible and UV light irradiation to induce photocatalytic water splitting. Most photocatalysts possess a large band gap and are therefore only responsive to UV irradiation. Solar irradiation consists of only 4-5% energy in the UV region but 45% in the visible region. Thus, while the idea of developing a visible light sensitive photocatalyst to perform water splitting is reasonable, a photocatalyst with a band structure that can absorb visible light irradiation and thermodynamically induce an overall water splitting reaction is not yet readily available. Therefore, band structure engineering has been applied to narrow the band gap of photocatalysts to construct a band structure that could induce the water splitting reaction.

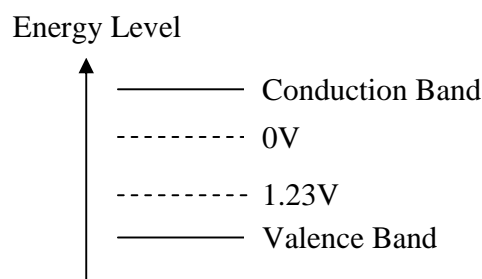


**Fig.1.** Energy structure of an effective photocatalyst for the overall water splitting reaction

Band engineering of semiconductors has been performed by adding a cocatalyst and dopants using various synthesis route. In general, band engineering distorts the crystal structure and modifies the band level of photocatalysts. A dopant that was initially a center of recombination for electron-hole pairs can act as an active site for water splitting reaction with appropriate modification. Currently, cationic and anionic modifications are the most popular methods to produce photocatalysts for overall water splitting purposes. Cationic additives are predominantly transition and noble metal ions with  $d^0$  or  $d^{10}$  electronic configurations, while anionic additives typically consist of nitrogen, sulfur and chlorine compounds. The combination of both modification types is also applicable to improve photocatalytic performance. This paper discusses cationic and anionic modifications of photocatalysts and their effects on band structure and photocatalytic water splitting.

## 2. CATIONIC MODIFICATION

Transition metals are predominantly used to modify the band structure of a semiconductor. Examples of cationic additives include Bi, Mo, Au, Rh, Zr, Pt, Ru, Cr, Ni, V, Fe, La, In and Ce.  $\text{TiO}_2$  is the most popular photocatalyst and has been widely modified by various cautions. A cocatalyst and dopants are incorporated into  $\text{TiO}_2$  rutile and anatase phase to narrow the  $\text{TiO}_2$  band gap, extending the absorption edge from the UV to visible light region. The Bi-doped  $\text{TiO}_2$  studied by Naik et al. is one example of a  $d^{10}$  cationic dopants for  $\text{TiO}_2$  [2]. This nano composite was synthesized using a soft chemical template free homogeneous co-precipitation method. A mesoporous compound formed with a significant red shift in the absorption edge was formed, indicating its capability of absorbing more lights with a longer wavelength. After calcination at  $400^\circ\text{C}$ , 4.3% of the apparent quantum efficiency was achieved at  $198.4 \mu\text{mol/h}$  of  $\text{H}_2$ .  $\text{TiO}_2$  films doped with Mo were prepared by Li et al. using the layer-by-layer method [3]. Optimum Mo doping enhanced the transformation from the anatase to the rutile phase and reduced the surface oxygen vacancies that could promote recombination of the photo induced charges. The doped  $\text{TiO}_2$  exhibited photocatalytic activity 3.3 times higher than the bare  $\text{TiO}_2$  because the introduction of  $\text{Mo}^{6+}$  resulted in a red shift of the absorption edge to the visible region.

In addition, the function of Au as a cocatalyst has been investigated by many researchers. Lin et al. deposited gold nanoparticles on  $\text{KTiNbO}_5$  using the deposition precipitation method [4]. Due to effective photo excited charge separation, the photo activity of 0.63wt% Au/ $\text{KTiNbO}_5$  with uniformly dispersed gold nanoparticles was 47 times higher than that of bare  $\text{KTiNbO}_5$ . Lunawat et al. studied a Au-doped CdS/SBA-15 photocatalyst [5]. In their study, Pt and Au dopants produced entirely different activity in CdS/SBA-15. The Au-doped CdS/SBA-15 exhibited decreased photo activity, while the Pt-doped CdS/SBA-15 exhibited a substantial increase

compared with the undoped CdS/SBA-15. The researchers explained that the surface properties, rather than the electronic structure, of their photocatalysts played an important role. An optimum crystallite size is crucial in avoiding active site blockage by metal particles. Feil et al. used a modified classical citrate method in synthesizing a gold impregnated  $\text{TiO}_2$  photocatalyst [6]. In their study, anodic oxidation of Ti metal in fluoride electrolytes containing gold nanoparticles was used to grow  $\text{TiO}_2$  nano tube arrays. Using methanol as a sacrificial reagent, the Au doped  $\text{TiO}_2$  nanotubes exhibited higher photocatalytic hydrogen production than the Au-free  $\text{TiO}_2$  nanotubes. Chiarello et al. prepared Au/ $\text{TiO}_2$  sample using flame spray pyrolysis [7]. At 1% Au doping, an additional absorption band was observed in the visible region. The absorption band was named the plasmonic absorption band and led to the purple color of the prepared photocatalyst. The resulting hydrogen evolution rate from photocatalytic water splitting was observed to be one order of magnitude higher than that of the undoped  $\text{TiO}_2$ . Rosseler et al. synthesized a Au/ $\text{TiO}_2$  photocatalyst using the sol-gel and subsequent direct anionic exchange process with various types of  $\text{TiO}_2$  and porogens [8]. Their study revealed that photocatalytic water splitting is affected by the type of metallic doping, surface properties, anatase/rutile ratio, metal-support interaction and amount of methanol. In fact, high  $\text{H}_2$  production efficiency ( $120 \mu\text{mol/min}$ ) was achieved over days without deactivation and with a low amount of methanol. Chen et al. prepared Au/ $\text{TiO}_2$  via the sodium citrate reduction method to study the effect of surface plasmon resonance (SPR) on photocatalytic water splitting using simulated solar irradiation [9]. The effect of the Au addition on  $\text{TiO}_2$  is illustrated in Fig.2. The Au particles act as electron traps and active sites to improve the hydrogen evolution activity. In addition, the intensified electric field at the interface between the Au particle and  $\text{TiO}_2$  contributes to enhanced water splitting activity when both UV and visible light irradiation were used. Nevertheless, no  $\text{H}_2$  evolution was observed when Au/ $\text{TiO}_2$  in pure water was irradiated with only visible light, which implies that the SPR effect from the gold particles is insufficient to produce the water splitting reaction. Comparing discussed research works, Au/ $\text{TiO}_2$  possess greater hydrogen evolution rate if sacrificial reagents like methanol was used.

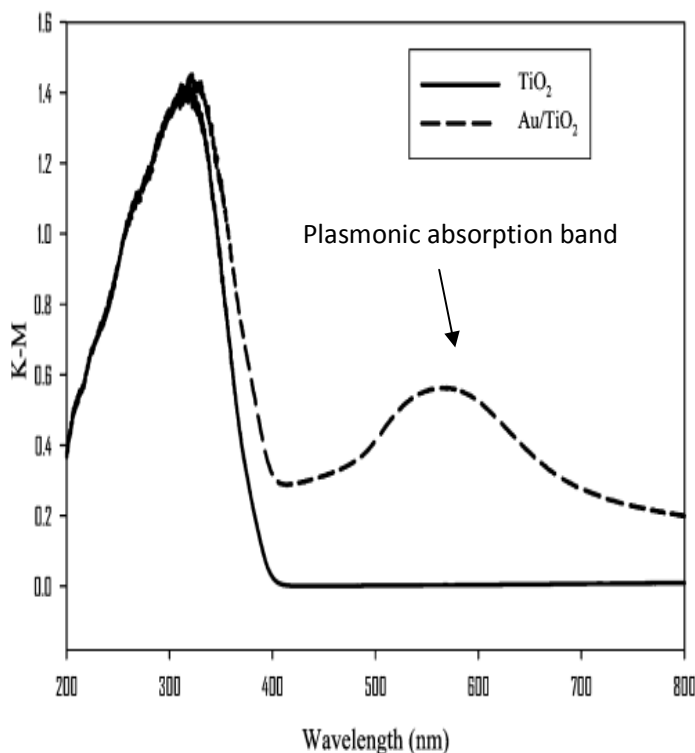


**Fig. 2.** Plasmonic absorption band derived from gold modification [9].

The d<sup>6</sup> electronic structure of rhodium (Rh) has also been studied intensively [10-17]. Detailed studies have demonstrated that (Ga<sub>1-x</sub>Zn<sub>x</sub>)(N<sub>1-x</sub>O<sub>x</sub>) is a promising visible light active photocatalyst [10, 14-17]. When doping (Ga<sub>1-x</sub>Zn<sub>x</sub>)(N<sub>1-x</sub>O<sub>x</sub>) with Rh, its photocatalytic activity was observed to increase. Nevertheless, because hydrogen and oxygen recombination occurred as they were catalyzed by Rh, Maeda et al. coated rhodium particled with chromium oxide, Rh-Cr<sub>2</sub>O<sub>3</sub> via photo deposition from aqueous metal precursors. The impregnation of chromium oxide successfully suppressed the recombination of hydrogen and oxygen. The resulting photocatalyst was able to produce hydrogen upon visible light irradiation. In addition to the work of Maeda et al., Rh doping has also been studied by Ma et al. [13] and Kumagai et al. [12]. Ma et al. studied potassium niobate nano scrolls doped with Rh nanoparticles [13]. These researchers used rhodium hydroxide as a precursor and prepared potassium niobate nano scrolls using solid calcinations. Their results indicated that 0.1wt% Rh yielded optimum water splitting activity with 1340 μmol/h per gram of photocatalyst. In addition, proton-exchange using 1M HCl and subsequent hydration has also been performed for the Rh doped photocatalyst. This procedure enhances the hydrogen evolution rate to 1480 μmol/h per gram of photocatalyst. Kumagai et al. prepared Rh<sup>3+</sup> doped ZnGa<sub>2</sub>O<sub>4</sub> using a hydrothermal method

[12]. All the metal precursors were firstly mixed in a nitric acid solution, and the resulting mixture was then combined with ammonia to reach pH 9. After stirring for two hours, the mixture was autoclaved at 80°C for 24 hours. After centrifugation and filtration, the resulting yellowish precipitates were washed with distilled water several times. Upon drying, Rh<sub>2</sub>O<sub>3</sub> was added using RhCl<sub>3</sub>·3H<sub>2</sub>O as the precursor via the impregnation method. Finally, calcination at 500°C for 1 hour was performed to obtain the photocatalyst. Rh doping shifted the absorption edge of ZnGa<sub>2</sub>O<sub>4</sub> into the visible light region. H<sub>2</sub> evolution in the presence of a sacrificial reagent under visible light irradiation (>500nm) confirmed the function of Rh<sub>2</sub>O<sub>3</sub> as the active site for H<sub>2</sub> evolution.

The use of ZrO<sub>2</sub> doping to enhance the photocatalytic activity of TaON has also been investigated [18-21]. TaOH has a suitable band potential and is stable under photo corrosion to act as a promising visible light driven photocatalyst. In these studies, TaON was prepared via nitridation of Ta<sub>2</sub>O<sub>5</sub> under a NH<sub>3</sub> flow at 1123K for 15 hours. Nevertheless, a high density of surface defects on TaON resulted in low activity of the photocatalyst. The surface defects acted as recombination centers for the photo generated electron-hole pairs. By incorporating ZrO<sub>2</sub> into the nitridation of Ta<sub>2</sub>O<sub>5</sub>, a highly crystalline ZrO<sub>2</sub>-TaON resulted and surface defect formation was suppressed. In addition, ZrO<sub>2</sub> suppresses the aggregation of particulate during nitridation, and aggregation causes a reduction in photocatalytic activity. Under the reducing atmosphere of NH<sub>3</sub>, reduced tantalum species formation (Ta<sup>3+</sup>) can be restrained by ZrO<sub>2</sub>, thereby causing it to become more cationic, and increasing the visible light absorption of the photocatalyst.

Pt has been applied to many types of catalytic reactions and appears to be a noble metal dopant that always enhances photocatalytic activity. Lin et al. employed the evaporation induced self assembly (EISA) method to prepare mesoporous Nb<sub>2</sub>O<sub>5</sub> [22]. Pt was then photo deposited as a cocatalyst into the framework of Nb<sub>2</sub>O<sub>5</sub>. The Pt/Nb<sub>2</sub>O<sub>5</sub> was reported to produce a high hydrogen evolution rate of 4647 μmol/g.h in UV light irradiated water splitting with methanol as the sacrificial reagent; this rate is much higher than that other metal doped Nb<sub>2</sub>O<sub>5</sub>. Well-dispersed Pt nanoparticles contributed to the efficient charge separation in the photocatalyst. Pt doping on TiO<sub>2</sub> was also intensively studied [23-27]. Ikuma et al. produced Pt on TiO<sub>2</sub> via hydrogen reduction, photocatalytic and formaldehyde reduction methods to decompose the precursor H<sub>2</sub>PtCl<sub>6</sub> into Pt particles [24]. Different levels of photocatalytic water splitting activity were observed for different deposition methods. The formaldehyde reduction method where a TiO<sub>2</sub> powder and H<sub>2</sub>PtCl<sub>6</sub> mixture was placed in a formaldehyde atmosphere at 400°C, was observed to yield the highest H<sub>2</sub> evolution rate. Pt particles were not detected by Transmission Electron Microscopy (TEM) for the formaldehyde reduced

Pt/TiO<sub>2</sub>, indicating that a fine or thin layer of Pt particles was deposited. The Pt particles could be detected if heated at 800°C because agglomeration occurs. A Ce<sup>3+</sup>/Ce<sup>4+</sup> shuttle charge UV-irradiated photocatalytic water splitting system using Pt/TiO<sub>2</sub> was studied by Kozlova et al. [26]. A Pt/TiO<sub>2</sub> photocatalyst was prepared using a soft chemical method with sodium borohydride reducing H<sub>2</sub>PtCl<sub>6</sub>. In a shuttle charge system, the hydrogen and oxygen evolution reactions occur at different photocatalyst particles, implying that hydrogen evolution and Ce<sup>3+</sup> oxidation occur at same particle and oxygen evolution and Ce<sup>4+</sup> reduction occur at another particle. This process reduces hydrogen and oxygen recombination and is capable of producing hydrogen of high purity, if the half reactions are performed separately in batches. Photocatalytic water splitting from visible light irradiation using Pt/TiO<sub>2</sub> was also studied using TiO<sub>2</sub> nanotube [23] and thin films [25]. Pt was incorporated into the TiO<sub>2</sub> nanotube matrix using an ion exchange method, and the highly dispersed Pt particles reduced the band gap of a bare TiO<sub>2</sub> nanotube from 3.1 to 2.48 eV. If the Pt was aggregately impregnated, the band gap reduction was not observed. The Pt/TiO<sub>2</sub> nanotube was visible light active and yielded hydrogen evolution rates of 2.3 and 14.6 μmol/h using pure water and methanol as sacrificial reagents, respectively. The Pt/TiO<sub>2</sub> thin film was however, prepared using the radio-frequency magnetron sputtering deposition (RF-MS) method and its absorption band was shifted into the visible range. Pt/TiO<sub>2</sub> thin films are applicable for photocatalytic water splitting with sacrificial reagent such as methanol and AgNO<sub>3</sub> solution using visible light with wavelengths longer than 550 nm.

RuO<sub>2</sub> doped photocatalysts have been studied by Inoue et al. [28-34]. In their report, RuO<sub>2</sub> and divalent ion (Zn<sup>2+</sup>, Mg<sup>2+</sup>) doped GaN were observed to be highly reactive and stable photocatalyst for overall water splitting under UV irradiation [28]. These photocatalysts were prepared by nitridation of sulfide precursors and impregnation of the resulting compounds with a Ru precursor, followed by calcinations. The undoped GaN produced little hydrogen with no oxygen; however, the doped GaN increased the hydrogen and oxygen evolution in a stoichiometric ratio. This study also revealed that RuO<sub>2</sub> with tetravalent ion (Si<sup>4+</sup>, Ge<sup>4+</sup>) doped GaN is not active for photocatalytic water splitting because tetravalent ions distort the crystal structure differently than divalent ions. The use of RuO<sub>2</sub> doped β-Ge<sub>3</sub>N<sub>4</sub> for overall water splitting has also been demonstrated [3]. In this study, sulfuric acid was observed to enhance the photocatalytic activity because the basic condition tends to hydrolyze the photocatalyst. Hydrolysis of the photocatalyst was observed to collapse the catalyst surface and loosen the interfacial contact between β-Ge<sub>3</sub>N<sub>4</sub> and RuO<sub>2</sub>, thus reducing the rate of H<sub>2</sub> and O<sub>2</sub> evolution as the reaction progressed. This study also demonstrated that regeneration of the photocatalyst can be achieved through calcinations and RuO<sub>2</sub> reloading to obtain 80%

of the initial activity. Subsequent studies of Inoue et al. have also been reported [31-32]. From Kadowaki et al. [31], inactive CeO<sub>2</sub> with an f<sup>0</sup>d<sup>0</sup> electronic configuration has been successfully activated by doping RuO<sub>2</sub> with Sr<sup>2+</sup>. The formation of Ce<sup>3+</sup>, which was the main reason for CeO<sub>2</sub> inactivity, was suppressed by the dopants by promotion of the formation of Ce<sup>4+</sup>. This study is the first example of lanthanide metal oxides as photocatalysts for an overall water splitting reaction. Another photocatalyst, RuO<sub>2</sub>-PbWO<sub>4</sub> was studied by Kadowaki et al. [32]. PbWO<sub>4</sub> was prepared via a solid state reaction from oxide precursors and subsequently impregnated with a Ru precursor, followed by calcinations. This photocatalyst with a combination d<sup>10</sup>s<sup>2</sup> (Pb<sup>2+</sup>)-d<sup>0</sup> (W) electronic configuration was more active towards UV irradiation compared with inactive WO<sub>3</sub>. The enhancement of the orbital dispersion by Pb<sup>2+</sup> was determined to be a crucial reason for the photo activity of this photocatalyst. A review of RuO<sub>2</sub> doped metal oxides and nitrides with d<sup>0</sup> and d<sup>10</sup> electronic configuration by Inoue et al. [30] has further clarified the role of dopants in Photocatalysis. It was concluded that distortion and unsymmetrical metal-oxygen octahedral/tetrahedral coordination increase the photocatalytic activity of d<sup>0</sup> and d<sup>10</sup> metal oxides. Further enhancement of photocatalytic activity can be achieved if divalent metal ions are incorporated in the electronic structure of the photocatalyst. This phenomenon occurs because divalent metal ions will contribute to a largely dispersed band and enhance the mobility of the photo excited electrons. In addition to the work by Inoue et al., the use of Ru as a cocatalyst has been reported by Navarro et al. [35]. A CdS-CdO-ZnO photocatalyst was prepared from sequential precipitation and Ru particles were photo deposited under visible light irradiation. The addition of Ru significantly increased the photo activity of CdS-CdO-ZnO. The interaction between RuO<sub>2</sub> and CdS reduces electron-hole recombination and subsequently enhances water splitting activity.

Maeda et al. have studied photocatalytic water splitting from solid solution (Ga<sub>1-x</sub>Zn<sub>x</sub>)(N<sub>1-x</sub>O<sub>x</sub>) using Rh/Cr<sub>2</sub>O<sub>3</sub> core/shell nanoparticles as cocatalyst [14-15, 17, 36]. Rh doped on (Ga<sub>1-x</sub>Zn<sub>x</sub>)(N<sub>1-x</sub>O<sub>x</sub>) did not promote photocatalytic water splitting because of the recombination of hydrogen and oxygen on the Rh particles. Coating Rh with Cr<sub>2</sub>O<sub>3</sub> suppressed the H<sub>2</sub>/O<sub>2</sub> recombination, subsequently enhancing the overall water splitting activity. Rh and Cr<sub>2</sub>O<sub>3</sub> were photodeposited in sequence on (Ga<sub>1-x</sub>Zn<sub>x</sub>)(N<sub>1-x</sub>O<sub>x</sub>) solid solutions using Na<sub>3</sub>RhCl<sub>6</sub>·2H<sub>2</sub>O and K<sub>2</sub>CrO<sub>4</sub> as precursors. This study also revealed that the core/shell structure of Rh/Cr has higher water splitting activity than Rh-Cr mixed oxides used as cocatalyst. Maeda et al. suggested that the core/shell structure yields more efficient electron transfer from the conduction band of (Ga<sub>1-x</sub>Zn<sub>x</sub>)(N<sub>1-x</sub>O<sub>x</sub>) to the Rh particle. This photocatalyst was observed to be stable at pH 4.5. A reactant pH study indicated that this photocatalyst would be corroded and hydrolyzed at pH 3.0 and 6.2. In addition to Maeda et al., the use of Cr in

photocatalyst preparation has also been demonstrated [37-39]. Liu et al. [39] prepared Cr/SrTiO<sub>3</sub> using a solvothermal method. Compared with bare SrTiO<sub>3</sub>, Cr/SrTiO<sub>3</sub> has greater UV irradiated photocatalytic activity. Cr/SrTiO<sub>3</sub> was also observed to be visible light responsive, which was attributed to the band transition from the Cr 3d to the Cr 3d+Ti 3d hybrid orbital. In addition, Cr-doping is also the main reason for the visible light sensitive Cr-doped Bi<sub>4</sub>Ti<sub>3</sub>O<sub>12</sub> prepared via the sol-gel route, as described in the work of Zhang et al. [38]. Cr<sub>2</sub>O<sub>3</sub> has also been used in the work of Zhang et al. to dope TiO<sub>2</sub> nanotubes [37]. The absorption spectrum is observed to extend into the visible light region, making the photocatalyst visible light active. Cr<sup>3+</sup> predominantly contributed to visible light water splitting activity by forming another valence band to reduce the band gap from 3.3 (TiO<sub>2</sub> nanotube) to 2.3 eV (Cr<sub>2</sub>O<sub>3</sub>/TiO<sub>2</sub> nanotube).

Nickel oxide is extensively doped with a perovskite type oxide to improve its photocatalytic water splitting activity by visible light irradiation. Jeong et al. synthesized NiO/Sr<sub>3</sub>Ti<sub>2</sub>O<sub>7</sub> from a solid state reaction method (SSRM) and a polymerized complex method (PCM) [40]. Impregnation of NiO has increased the photocatalytic activity of Sr<sub>3</sub>Ti<sub>2</sub>O<sub>7</sub> significantly. By comparison, PCM appears to be a better method to produce NiO/Sr<sub>3</sub>Ti<sub>2</sub>O<sub>7</sub> because of the resulting higher photo activity and stability towards prolonged irradiation. Visible light irradiation using NiO/K<sub>4</sub>Nb<sub>6</sub>O<sub>17</sub> prepared by Lin et al. via a two step solid state reaction was observed to exhibit higher photocatalytic water splitting compared with the unloaded K<sub>4</sub>Nb<sub>6</sub>O<sub>17</sub> catalyst and the NiO/K<sub>4</sub>Nb<sub>6</sub>O<sub>17</sub> prepared using a conventional impregnation method [41]. The researchers reported that NiO is well dispersed in the bulk structure of K<sub>4</sub>Nb<sub>6</sub>O<sub>17</sub> instead of the surface. Therefore, the shadowing effect caused by NiO is minimized, allowing more light absorption by the K<sub>4</sub>Nb<sub>6</sub>O<sub>17</sub>. In addition, photo generated electron transfer to NiO becomes more efficient. NiO was also doped into InTaO<sub>4</sub> by Chiou et al. [42]. In their study, InTaO<sub>4</sub> was prepared from a sol-gel method, instead of through a conventional solid state reaction method, such that a thin film of InTaO<sub>4</sub> was formed. InTaO<sub>4</sub> is a visible light sensitive material capable of splitting water under irradiation. Impregnating NiO increases the initial hydrogen evolution rate of InTaO<sub>4</sub> because Ni/NiO core/shell nanoparticles efficiently increase charge transfer and enhance the reduction of H<sup>+</sup> to hydrogen. Deactivation of NiO/InTaO<sub>4</sub> can occur when Ni(OH)<sub>2</sub> is formed. A similar indium photocatalyst, InVO<sub>4</sub> doped with NiO, was also synthesized by Lin et al. [43]. Highly crystallized InVO<sub>4</sub> was active in producing H<sub>2</sub> from visible light irradiation. Subsequent impregnation with NiO followed by reduction in H<sub>2</sub> and oxidation in O<sub>2</sub> produced NiO/InVO<sub>4</sub> with an ultra thin NiO layer and a metallic Ni core. Distribution of the photo generated electrons by the ultra thin structure contributed to a 40% increase in the photocatalytic activity. NiO impregnation via a reduction-oxidation process was also performed by Tang et al. to synthesize

NiO<sub>x</sub>/Sm<sub>2</sub>InTaO<sub>7</sub> [44]. This pyrochlore-type photocatalyst could produce H<sub>2</sub> from pure water under visible light irradiation. NiO loading distorted the lattice and formed a highly dispersed conduction band from a hybridized In 5s5p orbital. Band structure changes caused by the NiO loading were determined to be responsible for the high water splitting activity. A noble metal photocatalyst doped with NiO was presented by Wang et al. [45]. NiO/Ca<sub>2</sub>Fe<sub>2</sub>O<sub>5</sub> synthesized via the sol-gel and impregnation method was observed to be active in producing hydrogen from pure water, even though Ca<sub>2</sub>Fe<sub>2</sub>O<sub>5</sub> is not an active photocatalyst. By adding CO<sub>2</sub> and NaHCO<sub>3</sub> in the water splitting reaction, the hydrogen evolution rate further increased because hole scavenging was promoted and reduced charge recombination.

V doped K<sub>2</sub>La<sub>2</sub>Ti<sub>3</sub>O<sub>10</sub> was synthesized by Yang et al. via the sol gel method [46]. At an optimum V doping of 1.5%, increased photocatalytic hydrogen production was achieved under both UV and visible light radiation. Vanadium doping was observed to change the lattice parameter of K<sub>2</sub>La<sub>2</sub>Ti<sub>3</sub>O<sub>10</sub>, but the crystal structure remained unchanged. In addition, DRS demonstrated that visible light absorptive properties are improved and favorable for photocatalytic activity. Hybridization of the V3d electron orbit with the O2p electron orbit forms a new localized energy level that allows the photocatalyst to be excited at lower energy.

The performance of iron-doped Pt-TiO<sub>2</sub> nanotubes prepared via the sol gel method was analyzed by Eder et al. [47]. Improved photocatalytic activity by up to two orders of magnitude was observed for the prepared photocatalyst when compared with commercial TiO<sub>2</sub>. The authors claimed that the absorption edge of the photocatalyst shifted considerably into the visible light region and that this red shift resulted from the excitation of Fe<sup>3+</sup> 3d electrons into the conduction band of TiO<sub>2</sub>. Sasaki et al. loaded Fe<sub>2</sub>O<sub>3</sub> onto SrTiO<sub>3</sub>:Rh in a Z-scheme Photocatalysis system via the impregnation method [48]. However, in their work, the Fe<sub>2</sub>O<sub>3</sub> doped photocatalyst did not gain significant attention because the Ru doped photocatalyst exhibited superior activity.

Li et al. synthesized La-doped Bi<sub>2</sub>AlNbO<sub>7</sub> via a solid state reaction [49]. Their study revealed that lanthanum doping increased the band gap of Bi<sub>2</sub>AlNbO<sub>7</sub>. The conduction band defined by La 5d, Bi 6p and Nb 4d is observed to be more positive than that of undoped Bi<sub>2</sub>AlNbO<sub>7</sub>. The water splitting activity of Bi<sub>1.8</sub>La<sub>0.2</sub>AlNbO<sub>7</sub> was observed to be two times higher, which was attributed to the change in the band structure and La<sub>3+</sub> on the photocatalyst surface. However, Yan et al. studied the photocatalytic water splitting activity of La-doped NaTaO<sub>3</sub> prepared via microwave heating [50]. At 2% doping, La<sub>0.02</sub>Na<sub>0.98</sub>TaO<sub>3</sub> with good crystallinity and a high surface area was formed and possessed improved photocatalytic water splitting activity.

Hu et al. demonstrated  $\text{In}^{3+}$  incorporation into GaON via a hydrothermal and nitridation reaction [51]. GaON is visible light sensitive photocatalyst; however the introduction of  $\text{In}^{3+}$  further dispersed the hybridized orbitals, causing a red shift of the DRS absorption edge, in which the photocatalytic activity is improved. Wei et al. studied the photocatalytic activity of In-doped  $\text{H}_2\text{LaNb}_2\text{O}_7$  prepared via a solid state reaction [52]. Their study indicated that an optimum amount of In doping exists such that the thickness of the space charge layer is equal to the light penetration depth. This photocatalyst was sensitive to visible light and capable of producing hydrogen with sacrificial reagent.

Cerium doped zeolites were studied by Krishna et al. [53]. Zeolites alone are not active photocatalyst. By doping them with low amount of cerium, the interaction between  $\text{Ce}^{3+}$  and the support is responsive to irradiation to generate photoelectrons and water molecules could be split to produce hydrogen.

### 3. ANIONIC MODIFICATION

In general, oxide photocatalysts possess a large band gap that is unresponsive to visible light irradiation. (Oxy)nitride photocatalysts, however, have a narrower band gap and are responsive to visible light irradiation. The valence band of an (oxy)nitride photocatalyst consists of a N2p orbital that has a lower potential than the valence band of the oxide photocatalyst that is normally formed by the O2p orbital [54]. An (oxy) nitride photocatalyst, therefore has a broader absorption band in the visible region. Nevertheless, compared with an oxide photocatalyst, an (oxy)nitride photocatalyst is typically not thermally stable and undergoes photo corrosion. Several types of (oxy)nitride photocatalyst that have been under extensive research recently include GaN, GeN, perovskiteoxynitride, N- $\text{TiO}_2$  and TaON, and these are discussed in the following section.

Arai et al. demonstrated the preparation of GaN from  $\text{Ga}_2\text{S}_3$  using nitridation in a  $\text{NH}_3$  flow at 1273K for 15 hours [55]. The GaN formed was only active in the UV region. However, doping divalent ions such as  $\text{Zn}^{2+}$ ,  $\text{Mg}^{2+}$  and  $\text{Be}^{2+}$  could transform GaN into a visible light responsive material with high photocatalytic water splitting activity, and further enhancement could be achieved if  $\text{RuO}_2$  was present as a co-catalyst. Doping with a divalent ion was observed to increase the concentration and mobility of the holes. An N-doped GaO and ZnO solid solution was also studied by Parida et al. [56]. Prepared from a solid state reaction, the GaO-ZnO was added to different nitrogen precursors such as urea, glycine, hexamine and pyridine. N-doping reduced the band gap from 4.1 to 2.6 eV and extended the absorption band further into the visible light region. An apparent quantum efficiency of 5.1% by visible light irradiation was achieved using glycine as the N-precursor. Kamata et al. added into the oxynitride photocatalyst to form Ga-Zn-In oxynitride [57]. The absorption

edge of the photocatalyst reached 600 nm and the water molecules were photo catalytically split with suitable electron donors and acceptors. Although the photocatalyst was observed to be unstable in water oxidation reaction, modification with cobalt oxide stabilizes the system as an oxygen evolution promoter

Similarly to GaN, Ge has also used in the formation of (oxy) nitride photo catalyst. The synthesis of a photocatalyst from a solid solution of ZnO and GeN was performed by Takanabe et al., Wang et al. and Lee et al. [58-60]. They shared similar findings indicating that the absorption band in the visible light region was attributed to the valence band that consisted of hybridized Zn3d and N2p orbitals. The overall water splitting activity could be enhanced by doping metal ions such as Cu and Rh- $\text{Cr}_2\text{O}_3$ . The enhancement in activity was largely contributed to the high crystallinity because metal doping suppresses defect formation. A low defect concentration, which is also achievable through post calcinations after the nitridation process, is important in reducing the charge recombination. Nitridation of perovskite type materials has also been performed to synthesize visible light responsive photocatalysts. Hagiwara et al. synthesize N-doped  $\text{Pt/KTa}_{0.92}\text{Zr}_{0.08}\text{O}_3$  via  $\text{NH}_3$  nitridation [61]. The visible light inactive  $\text{Pt/KTa}_{0.92}\text{Zr}_{0.08}\text{O}_3$  was observed to split water molecules under visible light irradiation after nitrogen doping. The absorption edge of the photocatalyst extended from 350 to 600 nm upon nitrogen doping, which was attributed to the formation of  $\text{Ta}_3\text{N}_5$ . Perovskite niobium (oxy)nitrides were produced by Siritanaratkul et al. [62]. The photocatalytic water splitting of different types of perovskite type niobium oxynitrides such as  $\text{CaNbO}_2\text{N}$ ,  $\text{SrNbO}_2\text{N}$ ,  $\text{BaNbO}_2\text{N}$  and  $\text{LaNbON}_2$  were examined. Prepared via a polymerized complex method and ammonia nitridation, these photocatalysts exhibited a wide absorption band at high wavelengths (600-750 nm). The nitridation temperature appeared to be the dominant factor in producing photocatalysts with high water splitting activity. At lower temperature, the oxynitride phase was not properly formed, whereas at high temperature, reduced niobium species ( $\text{Nb}^{3+}$ ,  $\text{Nb}^{4+}$ ) that can act as charge recombination sites formed and caused lower activity.

$\text{TiO}_2$  is only sensitive to UV irradiation. However, several studies have demonstrated that through nitrogen doping, the absorption band of N- $\text{TiO}_2$  is extended deep into the visible light region. Yuan et al. prepared N- $\text{TiO}_2$  using urea as the nitrogen precursor [63]. They observed that the absorption edge was shifted up to 600 nm in the visible light region. Through XPS analysis, nitrogen was observed to present as chemisorbed  $\text{N}_2$  and substituted N. The substituted N was responsible for the visible light photocatalytic water splitting. Transformation from the anatase to the rutile phase was also observed to contribute to the activity. Sreethawong et al. studied the effect of the mesoporous structure of N- $\text{TiO}_2$  on the

visible light water splitting activity [64]. These researchers determined that the photocatalyst prepared from mesoporous  $\text{TiO}_2$  had higher activity compared with non-mesoporous  $\text{TiO}_2$ . Subsequently, Pt/N- $\text{TiO}_2$  was prepared to obtain higher photocatalytic activity [27]. Platinum doping remarkably increased the photo activity with an optimum loading of 1.3 wt%. In this photocatalytic system, good dispersion of platinum particles was significant to enhancing the water splitting activity. A  $d^0$ - $d^{10}$  complex photocatalyst,  $\text{Zn}_x\text{TiO}_y\text{N}_z$  was synthesized by Hisatomi et al. via the polymerized complex method [65]. The absorption band edge of this spinel-type oxynitride photo catalyst was extended to 550 nm, and water splitting occurred under visible light irradiation in a sacrificial reagent such as methanol and silver nitrate.

TaON has been studied considerably as a visible light photocatalyst. TaON can be produced from the nitridation of  $\text{Ta}_2\text{O}_5$ . However, due to its band position, TaON is only capable of producing hydrogen instead of the overall water splitting reaction, with low hydrogen evolution activity. Defects in the bulk and on the surface of TaON (reduced tantalum species) can act as electron-hole recombination centers that decrease photo activity. Post calcinations after nitridation is one approach to reduce the defects, but this approach is less appropriate because TaON is not thermally stable. Maeda et al. added  $\text{ZrO}_2$  to reduce the defects in the TaON structure via a solid state reaction [19-20]. The addition of monoclinic  $\text{ZrO}_2$  suppressed the reduction of the Ta species during nitridation at high temperature. Therefore, the hydrogen evolution reaction under visible light irradiation with sacrificial reagent was enhanced. Although TaON alone cannot perform overall water splitting, it can be coupled with a Z-scheme water splitting system with a shuttle redox mediator to perform the overall water splitting reaction. Higashi et al. utilized Pt-TaON (hydrogen evolution photocatalyst) and  $\text{RuO}_2$ -TaON (oxygen evolution photocatalyst) to produce the overall water splitting reaction with an  $\text{I}^-/\text{IO}_3^-$  shuttle redox mediator [66]. Although the activity was low with 0.1-0.2% apparent quantum efficiency, the photo catalyst was the first example of a  $d^0$  oxynitride photocatalyst. Another type of oxygen evolution photocatalyst, Pt- $\text{WO}_3$ , was used with Pt-TaON by Abe et al. in a similar system [67]. Better selectivity of water oxidation to  $\text{O}_2$  and reduction of  $\text{IO}_3^-$  to  $\text{I}^-$  was achieved even if the solution contained a high amount of  $\text{I}^-$ . In addition, the photocatalytic system yielded a steady water splitting reaction under weak acid or neutral conditions even under prolonged irradiation.

In addition to nitride photocatalyst, sulfide photocatalysts such as CdS and ZnS are another type of anionic doped photocatalysts that have gained significant attention in this research area. As demonstrated by Sathish et al. [68], CdS can be prepared by precipitation from  $\text{Na}_2\text{S}$  and  $\text{Cd}(\text{NO}_3)_2$ , followed by calcination. An activity of 450  $\mu\text{mol/g.h}$  was reported for the CdS prepared. Mesoporous CdS was also

prepared via ultrasonic mediated precipitation at room temperature to form a particle size 4-6 nm using zeolite as the template for precipitation [69]. These three methods form CdS particles with different particle sizes and surface areas. CdS prepared via the ultrasonic method yielded the highest UV irradiated water splitting activity. This result indicates that the water splitting activity can be correlated with particle size and surface area. CdS supported on MgO and  $\text{Al}_2\text{O}_3$  was also synthesized to study the effect of the support on photocatalytic water splitting. Depending on the CdS loading and template that formed the CdS, the hydrogen evolution was higher than for the unsupported CdS. In general, the MgO supported CdS exhibited higher photoactivity compared with the  $\text{Al}_2\text{O}_3$  supported CdS because of the basic nature of MgO. In addition, noble metal doping such as with Pt further enhances the hydrogen evolution rate to 14.15 mmol/g.h. CdS undergoes photocorrosion and therefore is not stable under prolonged light irradiation. By loading CdS on an appropriate support, the photocatalytic water splitting initiated by CdS can be enhanced without eluting  $\text{S}^{2-}$  into the reaction medium. Loading CdS on ZTP (zirconium titanium phosphate) was performed by Parida et al. to synthesize a visible light photocatalyst [70]. CdS-ZTP was synthesized via ion exchange and subsequent sulfurization with sodium sulfide, and 15wt% CdS-ZTP was observed to yield the highest hydrogen evolution rate with an apparent quantum efficiency of 5.84% using a sulfide solution as the sacrificial reagent. Choi et al. synthesize a Ni/NiO/ $\text{KNbO}_3$ /CdS nanocomposite for visible light hydrogen evolution in the presence of isopropanol [71]. At an appropriate amount of CdS and other components, enhanced hydrogen evolution was observed because charge recombination was suppressed in the reaction. CdS nanoparticles dispersed in SBA-15 observed by Lunawat et al. enhanced the photoactivity compared with bulk CdS [5]. SBA-15 was added to cadmium acetate in  $\text{H}_2\text{S}$  flow to form a CdS/SBA-15 photocatalyst. A subsequent study indicated that by doping CdS/SBA-15 with noble metals such as Pt, the hydrogen evolution reaction rate could be greatly enhanced to 800  $\mu\text{mol/g.h}$ . Shemesh et al. synthesize CdS-PdO and CdS-Pd<sub>4</sub>S via the aqueous condensation of  $\text{Pd}^{2+}$  onto CdS nanorods and high-temperature organic-phase synthesis, respectively [72]. Due to efficient charge separation, the hydrogen evolution rate of these photo catalysts was higher than that of bulk CdS with 3.25% apparent quantum efficiency being achieved. In addition, CdS has also been dispersed on a hydrophobic polymer sheet, as described in the work of Lunawat et al. [73]. Good adhesion of CdS nanoparticles on the polymer enabled the photocatalyst to perform long life photocatalytic water splitting. Separation of the photocatalyst and the reaction medium was much easier compared with the use of a powder photocatalyst. A polymer supported nanocomposite of CdS-ZnS was also studied by Deshpande et al. [74]. Good dispersion of nano-sized CdS particles in the range of 1-3 nm was achieved when ZnS was present to assist coating on polymer strip. Therefore, the water splitting

activity was increased because the hydrogen evolution rate was observed to be inversely proportional to the CdS particle size. CdS was also synthesized with ZnO and ZnS to form a hetero structure photocatalyst that was highly active in visible light driven hydrogen evolution. The photocatalyst  $(\text{ZnO})_2-(\text{ZnS})_1-(\text{CdS})_1$ , as reported by Wang et al. [75], yields a hydrogen evolution rate up to  $2790 \mu\text{mol/g.h}$  using  $\text{SO}_3^{2-}$  and  $\text{S}^{2-}$  ions as sacrificial reagents. Photoexcited electrons in this photocatalyst were also observed to have long lifetime ( $>225$  ns), which contribute to the production of hydrogen. Another study reported by Navarro et al. using a CdS-ZnO-CdO photocatalyst developed from sequential precipitation and thermal annealing investigated the photocatalytic hydrogen evolution [35]. Thermal treatment significantly affected the crystallinity and visible light absorption of the photocatalyst. Appropriate thermal treatment improved the physical charge separation and allowed more visible light of different wavelength to be absorbed. The addition of cocatalysts such as Ru and Pt enhanced the hydrogen evolution. Ru appeared to be a better candidate for the cocatalyst because  $\text{RuO}_2$  particles have better interaction with CdS particles, which reduces charge recombination.

In addition to the combination with CdS to form a photocatalyst, ZnS with a band gap of 3.6 eV is also a type of sulfide photocatalyst. Jang et al. synthesize mesoporous ZnS nano plates via a solvo thermal method using ethylenediamine and calcination [76]. In their study, the calcination temperature affected the hydrogen production but did not appear to be correlated with surface area. The rate of hydrogen evolution was observed to be highest for the mesoporous ZnS calcined at  $500^\circ\text{C}$ . Using ultrasonic spray pyrolysis (USP), Bang et al. developed ZnS:  $\text{Ni}^{2+}$  hollow microspheres and nanoparticles [77].  $\text{Ni}^{2+}$  formed a new energy level in the ZnS band structure that was capable of absorbing visible light to 550 nm. Nanoparticle ZnS:  $\text{Ni}^{2+}$  had higher hydrogen evolution activity than hollow microspheres regardless of the larger surface area, most likely due to charge recombination at their surface defects. Nevertheless, the researchers suggested that a balance between optimal crystallinity and surface area is necessary for photo excited electrons to induce photo oxidation at the photocatalyst surface. In addition, Wu et al. prepared  $(\text{AgIn})_x\text{Zn}_{2(1-x)}\text{S}_2$  solid solutions via a complete aqueous route [78]. A band gap between 2.11-2.45 eV and a broad absorption band in the visible region were reported. Hydrogen evolution in sacrificial reagents yielded a rate of  $680 \mu\text{mol/g.h}$  and the photoactivity was sustained for at least 100 hours. Highly visible light active porous ZnS- $\text{In}_2\text{S}_3$ -Cu nanospheres were produced by Li et al. via a facile one-pot solvothermal method [79]. Without adding a cocatalyst,  $\text{ZnIn}_{0.25}\text{Cu}_{0.02}\text{S}_{1.395}$  was prepared at  $180^\circ\text{C}$  for 18 h to achieve a  $360 \text{ mmol/g.h}$  hydrogen evolution rate and a 22.6% apparent quantum yield at 420 nm. Such excellent hydrogen evolution performance was attributed to the high surface area that could accommodate more active sites at the surface, a porous

structure that enhanced photo oxidation and photo reduction, and efficient charge separation. Cu also plays an important role because of its higher light absorption rate.

#### 4. FUTURE RESEARCH DIRECTION

Significant research has been performed to improve photocatalytic water splitting to produce hydrogen. However, the water splitting efficiency is not high enough for the emergence of a hydrogen economy via clean hydrogen production. The research concentrated on finding visible light responsive photocatalyst should be continued because of the higher solar energy content in the visible light region. The synthesis of inexpensive and efficient photocatalysts is crucial, and the photocatalyst must be produced in abundance to produce enough hydrogen to replace fossil fuels. Silicon appears to be the most abundant material with properties of a semiconductor and could provide direction in the search for usable photo catalysts. Limited research has been conducted on silicon based photocatalysts [80-82]. Nevertheless, great potential in silicon-based photocatalysts is foreseen to harvest solar energy, and more research should be performed. In addition, anionic modification appears to be a promising band engineering technology to harvest visible light from solar energy. Sulfide and oxy(nitride) photocatalysts should be further improved to achieve higher quantum efficiencies. Furthermore, various strategies such as the combination of anionic-cationic modification in photocatalyst synthesis and the application of a Z-scheme system for water splitting reactions could be used in creating the ultimate photocatalyst.

#### CONCLUSIONS

Cationic and anionic modification of semiconductors is successfully employed in band engineering using different types of preparation methods such as hydrothermal, solid state reactions and polymerized complex methods for the purpose of improving the photocatalytic water splitting reaction. Enhanced hydrogen evolution has been achieved by broadening absorption of the light wavelength, efficient charge separation and the formation of a new band level to facilitate the mechanism of the water splitting reaction. This review also indicates the trend of utilizing visible light irradiation in the water splitting reaction. Although the hydrogen rate is not yet comparable to that of UV light irradiation, visible light sensitive photocatalysts have greater potential because solar irradiation mostly consists of the visible spectrum. Further research should be performed concerning various strategies to enable a hydrogen economy to be realized as soon as possible before irreversible damage done onto environment by a fossil fuel based economy.



## ACKNOWLEDGMENTS

The authors wish to express appreciation to theMyBrain 15Programme, USM Short Term Grant (Grant No. 60311051) for the financial support provided.

## REFERENCES

- [1] Fujishima A, Honda K. Electrochemical photolysis of water at a semiconductor electrode. *Nature* 1972;238:37–38.
- [2] Naik B, Martha S, Parida KM. Facile fabrication of  $\text{Bi}_2\text{O}_3/\text{TiO}_{2-x}\text{N}_x$  nanocomposites for excellent visible light driven photocatalytic hydrogen evolution. *International Journal of Hydrogen Energy* 2011;36:2794–2802.
- [3] Li C, Zhang D, Jiang Z, Yao Z, Jia F. Mo-doped titania films: preparation, characterization and application for splitting water. *New Journal of Chemistry* 2011;35:423–429.
- [4] Lin HY, Chang YS. Photocatalytic water splitting for hydrogen production on  $\text{Au}/\text{KTiNbO}_5$ . *International Journal of Hydrogen Energy* 2010;35:8463–8471.
- [5] Lunawat PS, Kumar R, Gupta NM. Structure sensitivity of nano-structured  $\text{CdS}/\text{SBA-15}$  containing Au and Pt co-catalysts for the photocatalytic splitting of water. *Catalysis Letter* 2008;121:226–233.
- [6] Feil AF, Migowski P, Scheffer FR, Pierozan MD, Corsetti RR, Rodrigues M, et al. Growth of  $\text{TiO}_2$  nanotube arrays with simultaneous Au nanoparticles impregnation: photocatalysts for hydrogen production. *Journal of Brazilian Chemical Society* 2010;21:1359–1365.
- [7] Chiarello GL, Selli E, Forni L. Photocatalytic hydrogen production over flame spray pyrolysis-synthesised  $\text{TiO}_2$  and  $\text{Au}/\text{TiO}_2$ . *Applied Catalysis B: Environment* 2008;84:332–339.
- [8] Rosseler O, Shankar MV, Du MKL, Schmidlin L, Keller N, Keller V. Solar light photocatalytic hydrogen production from water over Pt and  $\text{Au}/\text{TiO}_2$  (anatase/rutile) photocatalysts: influence of noble metal and porogen promotion. *Journal of Catalysis* 2010;269:179–190.
- [9] Chen JJ, Wu JCS, Wu PC, Tsai DP. Plasmonic photocatalyst for  $\text{H}_2$  evolution in photocatalytic water splitting. *The Journal of Physical Chemistry C* 2011;115:210–216.
- [10] Hisatomi T, Maeda K, Takanabe K, Kubota J, Domen K. Aspects of the water splitting mechanism on  $(\text{Ga}_{1-x}\text{Zn}_x)(\text{N}_{1-x}\text{O}_x)$  photocatalyst modified with  $\text{Rh}_{2-y}\text{Cr}_y\text{O}_3$  cocatalyst. *The Journal of Physical Chemistry C* 2009;113:21458–21466.
- [11] Hisatomi T, Miyazaki K, Takanabe K, Maeda K, Kubota J, Sakata Y, et al. Isotopic and kinetic assessment of photocatalytic water splitting on Zn-added  $\text{Ga}_2\text{O}_3$  photocatalyst loaded with  $\text{Rh}_{2-y}\text{Cr}_y\text{O}_3$  cocatalyst. *Chemical Physics Letter* 2010;486:144–146.
- [12] Kumagai N, Ni L, Irie H. A visible-light-sensitive water splitting photocatalyst composed of  $\text{Rh}^{3+}$  in a  $4d^6$  electronic configuration,  $\text{Rh}^{3+}$ -doped  $\text{ZnGa}_2\text{O}_4$ . *Chemical Communications* 2011;47:1884–1886.
- [13] Ma R, Kobayashi Y, Youngblood WJ, Mallouk TE. Potassium niobate nanoscrolls incorporating rhodium hydroxide nanoparticles for photocatalytic hydrogen evolution. *Journal of Material Chemistry* 2008;18:5982–5985.
- [14] Maeda K, Lu D, Teramura K, Domen K. Simultaneous photodeposition of rhodium-chromium nanoparticles on a semiconductor powder: structural characterization and application to photocatalytic overall water splitting. *Energy & Environmental Science* 2010;3:471–478.
- [15] Maeda K, Teramura K, Lu D, Saito N, Inoue Y, Domen K. Roles of  $\text{Rh}/\text{Cr}_2\text{O}_3$  (core/shell) nanoparticles photodeposited on visible-light-responsive  $(\text{Ga}_{1-x}\text{Zn}_x)(\text{N}_{1-x}\text{O}_x)$  solid solutions in photocatalytic overall water splitting. *The Journal of Physical Chemistry C* 2007;111:7554–7560.
- [16] Maeda K, Teramura K, Lu D, Takata T, Saito N, Inoue Y, et al. Characterization of Rh-Cr mixed-oxide nanoparticles dispersed on  $(\text{Ga}_{1-x}\text{Zn}_x)(\text{N}_{1-x}\text{O}_x)$  as a cocatalyst for visible-light-driven overall water splitting. *The Journal of Physical Chemistry B* 2006;110:13753–13758.
- [17] Maeda K, Teramura K, Masuda H, Takata T, Saito N, Inoue Y, et al. Efficient overall water splitting under visible-light irradiation on  $(\text{Ga}_{1-x}\text{Zn}_x)(\text{N}_{1-x}\text{O}_x)$  dispersed with Rh-Cr mixed-oxide nanoparticles: effect of reaction conditions on photocatalytic activity. *The Journal of Physical Chemistry B* 2006;110:13107–13112.
- [18] Kang KS, Kim CH, Park CS, Kim JW. Hydrogen reduction and subsequent water splitting of Zr-added  $\text{CeO}_2$ . *Journal of Industrial and Engineering Chemistry* 2007;13:657–663.
- [19] Maeda K, Terashima H, Kase K, Domen K. Nanoparticulate precursor route to fine particles of TaON and  $\text{ZrO}_2$ -TaON solid solution and their photocatalytic activity for hydrogen evolution under visible light. *Applied Catalysis A: General* 2009;357:206–212.
- [20] Maeda K, Terashima H, Kase K, Higashi M, Tabata M, Domen K. Surface modification of TaON with monoclinic  $\text{ZrO}_2$  to produce a composite photocatalyst with enhanced hydrogen evolution activity under visible light. *Bulletin of the Chemical Society of Japan* 2008;81:927–937.
- [21] Kumar P, Sharma P, Shrivastav R, Dass S, Satsangi VR. Electrodeposited zirconium-doped  $\alpha\text{-Fe}_2\text{O}_3$  thin film for photoelectrochemical water splitting. *International Journal of Hydrogen Energy* 2011;36:2777–2784.
- [22] Lin HY, Yang HC, Wang WL. Synthesis of mesoporous  $\text{Nb}_2\text{O}_5$  photocatalysts with Pt, Au, Cu and NiO cocatalyst for water splitting. *Catalysis Today*. 2011; 174: 106–113.
- [23] Alam Khan M, Shaheer Akhtar M, Woo SI, Yang OB. Enhanced photoresponse under visible light in Pt ionized  $\text{TiO}_2$  nanotube for the photocatalytic splitting of water. *Catalysis Communications* 2008;10:1–5.
- [24] Ikuma Y, Bessho H. Effect of Pt concentration on the production of hydrogen by a  $\text{TiO}_2$  photocatalyst. *International Journal of Hydrogen Energy* 2007;32:2689–2692.
- [25] Kitano M, Takeuchi M, Matsuoka M, Thomas JM, Anpo M. Photocatalytic water splitting using Pt-loaded visible light-responsive  $\text{TiO}_2$  thin film photocatalysts. *Catalysis Today* 2007;120:133–138.

- [26] Kozlova EA, Korobkina TP, Vorontsov AV. Overall water splitting over Pt/TiO<sub>2</sub> catalyst with Ce<sup>3+</sup>/Ce<sup>4+</sup> shuttle charge transfer system. *International Journal of Hydrogen Energy* 2009;34:138–146.
- [27] Sreethawong T, Laehsatee S, Chavadej S. Use of Pt/N-doped mesoporous-assembled nanocrystalline TiO<sub>2</sub> for photocatalytic H<sub>2</sub> production under visible light irradiation. *Catalysis Communications* 2009;10:538–543.
- [28] Arai N, Saito N, Nishiyama H, Inoue Y, Domen K, Sato K. Overall water splitting by RuO<sub>2</sub>-dispersed divalent-ion-doped GaN photocatalysts with d<sup>10</sup> electronic configuration. *Chemistry Letters* 2006;35:796–797.
- [29] Arai N, Saito N, Nishiyama H, Shimodaira Y, Kobayashi H, Inoue Y, et al. Overall water splitting by RuO<sub>2</sub>-loaded hexagonal YInO<sub>3</sub> with a distorted trigonal bipyramid. *Chemistry Letters* 2008;37:46–47.
- [30] Inoue Y. Photocatalytic water splitting by RuO<sub>2</sub>-loaded metal oxides and nitrides with d<sup>0</sup>- and d<sup>10</sup>-related electronic configurations. *Energy & Environmental Science* 2009;2:364–386.
- [31] Kadowaki H, Saito N, Nishiyama H, Inoue Y. RuO<sub>2</sub>-loaded Sr<sup>2+</sup>-doped CeO<sub>2</sub> with d<sup>0</sup> electronic configuration as a new photocatalyst for overall water splitting. *Chemistry Letters* 2007;36:440–441.
- [32] Kadowaki H, Saito N, Nishiyama H, Kobayashi H, Shimodaira Y, Inoue Y. Overall splitting of water by RuO<sub>2</sub>-loaded PbWO<sub>4</sub> photocatalyst with d<sup>10</sup>s<sup>2</sup>-d<sup>0</sup> configuration. *The Journal of Physical Chemistry C* 2007;111:439–444.
- [33] Maeda K, Saito N, Daling L, Inoue Y, Domen K. Photocatalytic properties of RuO<sub>2</sub>-loaded β-Ge<sub>3</sub>N<sub>4</sub> for overall water splitting. *The Journal of Physical Chemistry C* 2007;111:4749–4755.
- [34] Nishiyama H, Kobayashi H, Inoue Y. Effects of distortion of metal-oxygen octahedra on photocatalytic water-splitting performance of RuO<sub>2</sub>-loaded niobium and tantalum phosphate bronzes. *ChemSusChem* 2011;4:208–215.
- [35] Navarro RM, del Valle F, Fierro JLG. Photocatalytic hydrogen evolution from CdS-ZnO-CdO systems under visible light irradiation: effect of thermal treatment and presence of Pt and Ru cocatalysts. *International Journal of Hydrogen Energy* 2008;33:4265–4273.
- [36] Maeda K, Teramura K, Lu D, Saito N, Inoue Y, Domen K. Noble-metal/Cr<sub>2</sub>O<sub>3</sub> core/shell nanoparticles as a cocatalyst for photocatalytic overall water splitting. *Angewandte Chemie International Edition* 2006;45:7806–7809.
- [37] Zhang YJ, Wang YC, Yan W, Li T, Li S, Hu YR. Synthesis of Cr<sub>2</sub>O<sub>3</sub>/TNTs nanocomposite and its photocatalytic hydrogen generation under visible light irradiation. *Applied Surface Science* 2009;255:9508–9511.
- [38] Zhang H, Chen G, Li X. Synthesis and visible light photocatalysis water splitting property of chromium-doped Bi<sub>4</sub>Ti<sub>3</sub>O<sub>12</sub>. *Solid State Ionics* 2009;180:1599–1603.
- [39] Liu JW, Chen G, Li ZH, Zhang ZG. Electronic structure and visible light photocatalysis water splitting property of chromium-doped SrTiO<sub>3</sub>. *Journal of Solid State Chemistry* 2006;179:3704–3708.
- [40] Jeong H, Kim T, Kim D, Kim K. Hydrogen production by the photocatalytic overall water splitting on NiO/Sr<sub>3</sub>Ti<sub>2</sub>O<sub>7</sub>: effect of preparation method. *International Journal of Hydrogen Energy* 2006;31:1142–1146.
- [41] Lin HY, Lee TH, Sie CY. Photocatalytic hydrogen production with nickel oxide intercalated K<sub>4</sub>Nb<sub>6</sub>O<sub>17</sub> under visible light irradiation. *International Journal of Hydrogen Energy* 2008;33:4055–4063.
- [42] Chiou YC, Kumar U, Wu JCS. Photocatalytic splitting of water on NiO/InTaO<sub>4</sub> catalysts prepared by an innovative sol-gel method. *Applied Catalysis A: General* 2009;357:73–78.
- [43] Lin HY, Chen YF, Chen YW. Water splitting reaction on NiO/InVO<sub>4</sub> under visible light irradiation. *International Journal of Hydrogen Energy* 2007;32:86–92.
- [44] Tang X, Ye H, Liu H, Ma C, Zhao Z. Photocatalytic splitting of water under visible-light irradiation over the NiO<sub>x</sub>-loaded Sm<sub>2</sub>InTaO<sub>7</sub> with 4<sup>f</sup>-d<sup>10</sup>-d<sup>0</sup> configuration. *Journal of Solid State Chemistry* 2010;183:192–197.
- [45] Wang Y, Gao Y. Photocatalytic H<sub>2</sub> evolution from water in the presence of carbon dioxide over NiO/Ca<sub>2</sub>Fe<sub>2</sub>O<sub>5</sub>. *Reaction Kinetics, Mechanisms and Catalysis* 2010;99:485–491.
- [46] Yang Y, Chen Q, Yin Z, Li J. Study on the photocatalytic activity of K<sub>2</sub>La<sub>2</sub>Ti<sub>3</sub>O<sub>10</sub> doped with vanadium (V). *Journal of Alloys and Compounds* 2009;488:364–369.
- [47] Eder D, Motta M, Windle AH. Iron-doped Pt-TiO<sub>2</sub> nanotubes for photo-catalytic water splitting. *Nanotechnology* 2009;20: 055602.
- [48] Sasaki Y, Iwase A, Kato H, Kudo A. The effect of co-catalyst for Z-scheme photocatalysis systems with an Fe<sup>3+</sup>/Fe<sup>2+</sup> electron mediator on overall water splitting under visible light irradiation. *Journal of Catalysis* 2008;259:133–137.
- [49] Li Y, Chen G, Zhang H, Li Z. Electronic structure and photocatalytic water splitting of lanthanum-doped Bi<sub>2</sub>AlNbO<sub>7</sub>. *Materials Research Bulletin* 2009;44:741–746.
- [50] Yan SC, Wang ZQ, Li ZS, Zou ZG. Photocatalytic activities for water splitting of La-doped-NaTaO<sub>3</sub> fabricated by microwave synthesis. *Solid State Ionics* 2009;180:1539–1542.
- [51] Hu CC, Lee YL, Teng H. Influence of indium doping on the activity of gallium oxynitride for water splitting under visible light irradiation. *The Journal of Physical Chemistry C* 2011;115:2805–2811.
- [52] Wei Y, Li J, Huang Y, Huang M, Lin J, Wu J. Photocatalytic water splitting with In-doped H<sub>2</sub>LaNb<sub>2</sub>O<sub>7</sub> composite oxide semiconductors. *Solar Energy Materials and Solar Cells* 2009;93:1176–1181.
- [53] Krishna Reddy J, Suresh G, Hymavathi CH, Durga Kumari V, Subrahmanyam M. Ce (III) species supported zeolites as novel photocatalysts for hydrogen production from water. *Catalysis Today* 2009;141:89–93.
- [54] Maeda K, Domen K. Oxynitride materials for solar water splitting. *MRS Bulletin* 2011;36:25–31.

- [55] Arai N, Saito N, Nishiyama H, Domen K, Kobayashi H, Sato K, et al. Effects of divalent metal ion ( $\text{Mg}^{2+}$ ,  $\text{Zn}^{2+}$  and  $\text{Be}^{2+}$ ) doping on photocatalytic activity of ruthenium oxide-loaded gallium nitride for water splitting. *Catalysis Today* 2007;129:407–413.
- [56] Parida KM, Martha S, Das DP, Biswal N. Facile fabrication of hierarchical N-doped GaZn mixed oxides for water splitting reactions. *Journal of Materials Chemistry* 2010;20:7144–7149.
- [57] Kamata K, Maeda K, Lu D, Kako Y, Domen K. Synthesis and photocatalytic activity of gallium-zinc-indium mixed oxynitride for hydrogen and oxygen evolution under visible light. *Chemical Physics Letters* 2009;470:90–94.
- [58] Takanabe K, Uzawa T, Wang X, Maeda K, Katayama M, Kubota J, et al. Enhancement of photocatalytic activity of zinc-germanium oxynitride solid solution for overall water splitting under visible irradiation. *Dalton Transactions* 2009;45:10055–10062.
- [59] Wang X, Maeda K, Lee Y, Domen K. Enhancement of photocatalytic activity of  $(\text{Zn}_{1-x}\text{Ge})(\text{N}_2\text{O}_x)$  for visible-light-driven overall water splitting by calcination under nitrogen. *Chemical Physics Letters* 2008;457:134–136.
- [60] Lee Y, Teramura K, Hara M, Domen K. Modification of  $(\text{Zn}_{1-x}\text{Ge})(\text{N}_2\text{O}_x)$  solid solution as a visible light driven photocatalyst for overall water splitting. *Chemistry of Materials* 2007;19:2120–2127.
- [61] Hagiwara H, Kumagai K, Ishihara T. Effects of nitrogen doping on photocatalytic water-splitting activity of  $\text{Pt}/\text{KTa}_{0.92}\text{Zr}_{0.08}\text{O}_3$  perovskite oxide catalyst. *Chemistry Letters* 2010;39:498–499.
- [62] Siritanaratkul B, Maeda K, Hisatomi T, Domen K. Synthesis and photocatalytic activity of perovskite niobium oxynitrides with wide visible-light absorption bands. *ChemSusChem* 2011;4:74–78.
- [63] Yuan J, Chen M, Shi J, Shangguan W. Preparations and photocatalytic hydrogen evolution of N-doped  $\text{TiO}_2$  from urea and titanium tetrachloride. *International Journal of Hydrogen Energy* 2006;31:1326–1331.
- [64] Sreethawong T, Laehsatee S, Chauadej S. Comparative investigation of mesoporous- and non-mesoporous-assembled  $\text{TiO}_2$  nanocrystals for photocatalytic  $\text{H}_2$  production over N-doped  $\text{TiO}_2$  under visible light irradiation. *International Journal of Hydrogen Energy* 2008;33:5947–5957.
- [65] Hisatomi T, Hasegawa K, Teramura K, Takata T, Hara M, Domen K. Zinc and titanium spinel oxynitride ( $\text{Zn}_x\text{TiO}_y\text{N}_z$ ) as a  $d^0$ - $d^{10}$  complex photocatalyst with visible light activity. *Chemistry Letters* 2007;36:558–559.
- [66] Higashi M, Abe R, Ishikawa A, Takata T, Ohtani B, Domen K. Z-scheme overall water splitting on modified-TaON photocatalysts under visible light ( $\lambda < 500$  nm). *Chemistry Letters* 2008;37:138–139.
- [67] Abe R, Higashi M, Domen K. Overall water splitting under visible light through a two-step photoexcitation between TaON and  $\text{WO}_3$  in the presence of an iodate-iodide shuttle redox mediator. *ChemSusChem* 2011;4:228–237.
- [68] Sathish M, Viswanathan B, Viswanath RP. Alternate synthetic strategy for the preparation of CdS nanoparticles and its exploitation for water splitting. *International Journal of Hydrogen Energy* 2006;31:891–898.
- [69] Sathish M, Viswanath RP. Photocatalytic generation of hydrogen over mesoporous CdS nanoparticle: Effect of particle size, noble metal and support. *Catalysis Today* 2007;129:421–427.
- [70] Parida KM, Biswal N, Das DP, Martha S. Visible light response photocatalytic water splitting over CdS-pillared zirconium-titanium phosphate (ZTP). *International Journal of Hydrogen Energy* 2010;35:5262–5269.
- [71] Choi J, Ryu SY, Balcerski W, Lee TK, Hoffmann MR. Photocatalytic production of hydrogen on  $\text{Ni}/\text{NiO}/\text{KNbO}_3/\text{CdS}$  nanocomposites using visible light. *Journal of Materials Chemistry* 2008;18:2371–2378.
- [72] Shemesh Y, MacDonald JE, Menagen G, Banin U. Synthesis and photocatalytic properties of a family of CdS-PdX hybrid nanoparticles. *Angewandte Chemie International Edition* 2011;50:1185–1189.
- [73] Lunawat PS, Senapati S, Kumar R, Gupta NM. Visible light-induced splitting of water using CdS nanocrystallites immobilized over water-repellant polymeric surface. *International Journal of Hydrogen Energy* 2007;32:2784–2790.
- [74] Deshpande A, Shah P, Gholap RS, Gupta NM. Interfacial and physico-chemical properties of polymer-supported CdS-ZnS nanocomposites and their role in the visible-light mediated photocatalytic splitting of water. *Journal of Colloid and Interface Science* 2009;333:263–268.
- [75] Wang X, Liu G, Chen ZG, Li F, Lu GQ, Cheng HM. Highly efficient  $\text{H}_2$  evolution over ZnO-ZnS-CdS heterostructures from an aqueous solution containing  $\text{SO}_3^{2-}$  and  $\text{S}^{2-}$  ions. *Journal of Materials Research* 2010;25:39–44.
- [76] Jang JS, Yu CJ, Choi SH, Ji SM, Kim ES, Lee JS. Topotactic synthesis of mesoporous ZnS and ZnO nanoplates and their photocatalytic activity. *Journal of Catalysis* 2008;254:144–155.
- [77] Bang JH, Helmich RJ, Suslick KS. Nanostructured ZnS: $\text{Ni}^{2+}$  photocatalysts prepared by ultrasonic spray pyrolysis. *Advanced Materials* 2008;20:2599–2603.
- [78] Wu CC, Cho HF, Chang WS, Lee TC. A simple and environmentally friendly method of preparing sulfide photocatalyst. *Chemical Engineering Science* 2010;65:141–147.
- [79] Li Y, Chen G, Wang Q, Wang X, Zhou A, Shen Z. Hierarchical ZnS- $\text{In}_2\text{S}_3$ -CuS nanospheres with nanoporous structure: Facile synthesis, growth mechanism, and excellent photocatalytic activity. *Advanced Functional Materials* 2010;20:3390–3398.
- [80] Bahruji H, Bowker M, Davies PR. Photoactivated reaction of water with silicon nanoparticles. *International Journal of Hydrogen Energy* 2009;34:8504–8510.
- [81] Ryu SY, Balcerski W, Lee TK, Hoffmann MR. Photocatalytic production of hydrogen from water with visible light using hybrid catalysts of CdS attached to microporous

and mesoporous silicas. TheJournal of Physical Chemistry C 2007;111:18195–18203.

[82] Zhang RQ, Liu XM, Wen Z, Jiang Q. Prediction of silicon nanowires as photocatalysts for water splitting: Band structures calculated using density functional theory. TheJournal of Physical Chemistry C 2011;115:3425–3428.